Erschienen in: Nano Letters ; 16 (2016), 8. - S. 4960-4967
https://dx.doi.org/10.1021/acs.nanolett.6b01595

Large Magnetoresistance in Single-Radical Molecular Junctions

Ryoma Hayakawa,*[,†,§] Mohammad Amin Karimi,[†] Jannic Wolf,[‡] Thomas Huhn,[‡] Martin Sebastian Zöllner,[∥] Carmen Herrmann,[∥] and Elke Scheer*[,†]

[†]Department of Physics and [‡]Department of Chemistry, University of Konstanz, 78457 Konstanz, Germany

[§]International Center for Materials Nanoarchitectonics (WPI MANA), National Institute for Materials Science, 1 1 Namiki, Tsukuba 305 0044, Japan

[∥]Institute for Inorganic and Applied Chemistry, University of Hamburg, Martin Luther King Platz 6, 20146 Hamburg, Germany

ABSTRACT: Organic radicals are promising building blocks for molecular spintronics. Little is known about the role of unpaired electrons for electron transport at the single molecule level. Here, we examine the impact of magnetic fields on electron transport in single oligo(p phenyleneethynylene) (OPE) based radical mo lecular junctions, which are formed with a mechanically controllable break junction technique at a low temperature of 4.2 K. Surprisingly huge positive magnetoresistances (MRs) of 16 to 287% are visible for a magnetic field of 4 T, and the values are at least 1 order of magnitude larger than those of the analogous pristine OPE (2−4%). Rigorous analysis of the MR and of current−voltage and inelastic electron tunneling spectroscopy measurements reveal an effective reduction of the electronic coupling between the current carrying molecular orbital and the electrodes with increasing magnetic field. We suggest that the large MR for the single radical molecular junctions might be ascribed to a loss of phase coherence of the charge carriers induced by the magnetic field. Although further investigations are required to reveal the mechanism underlying the strong MR, our findings provide a potential approach for tuning charge transport in metal molecule junctions with organic radicals.

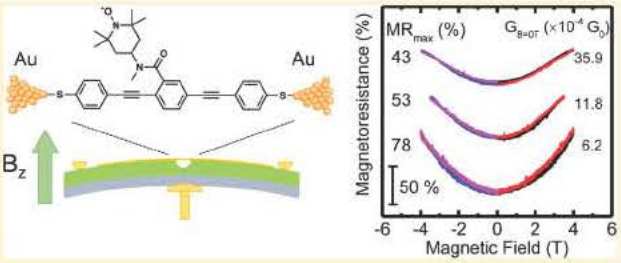

KEYWORDS: *Single organic radicals, large magnetoresistance, charge transport, mechanically controllable break junction*

Molecule based spintronics, which combines the molec ular spin degree of freedom with molecular electronics, has attracted considerable attention for exploiting functional logic and memory devices through a bottom up process.[1−7] Purely organic radicals, which consist of light elements such as H, C, N, O, and S, are promising materials for device applications.[8−10] The reason is that these molecules possess low spin−orbit coupling due to the light component elements, as opposed to, e.g., many transition metal complexes.[11,12] This property is expected to realize long spin relaxation times in the radical molecules, which is beneficial for molecular spintronics devices. Furthermore, the magnetism induced by localized magnetic moments, which originates from unpaired electrons, leads to versatile magnetic properties such as paramagnetic, ferromagnetic, and antiferromagnetic behaviors.[13−16] Such spin systems reveal physical aspects that differ fundamentally from bulk materials built up from spin polarized molecules. Little is known about the impact of magnetic moments on the charge transports in radical molecules at the single molecule level, in contrast to the many reported results on 3d spins in magnetic molecules containing transition metal atoms.[17−20]

Some examples have recently been reported on the interaction between localized electronic moments and con duction electrons, the so called Kondo resonance, in single radical molecules by means of scanning tunneling spectroscopy (STS) and the mechanically controllable break junction technique (MCBJ).[21−24] Several stable radical molecules, including nitronyl nitroxide radicals,[19] verdazyl radicals,[20] and phenylmethyl radicals,[22] were employed in these studies. In all cases, obvious Kondo resonance peaks were observed, thus demonstrating that unpaired electrons act as spin impurities. However, so far the detection of a Kondo resonance remains their only manifestation in single radical molecular junctions. Much less attention has been paid to other charge transport phenomena such as magnetoresistance (MR) effects and magnetic field induced variation of inelastic electron tunneling (IET), whereas abundant results have been reported for transition metal complexes.[25−28] Further understanding of the role of unpaired electrons in radical molecules and the manipulation of charge transport are challenging requirements.

In this letter, we evaluate the charge transport properties in single radical molecules by a MCBJ technique at a low temperature of 4.2 K under magnetic fields perpendicular to the transport direction (Figure 1a). In this study, stable and neutral radical molecules based on an oligo(*p* phenyleneethy nylene) (OPE) backbone, {4 [{[2,5 bis(4 sulfanylphenyl[eth 1

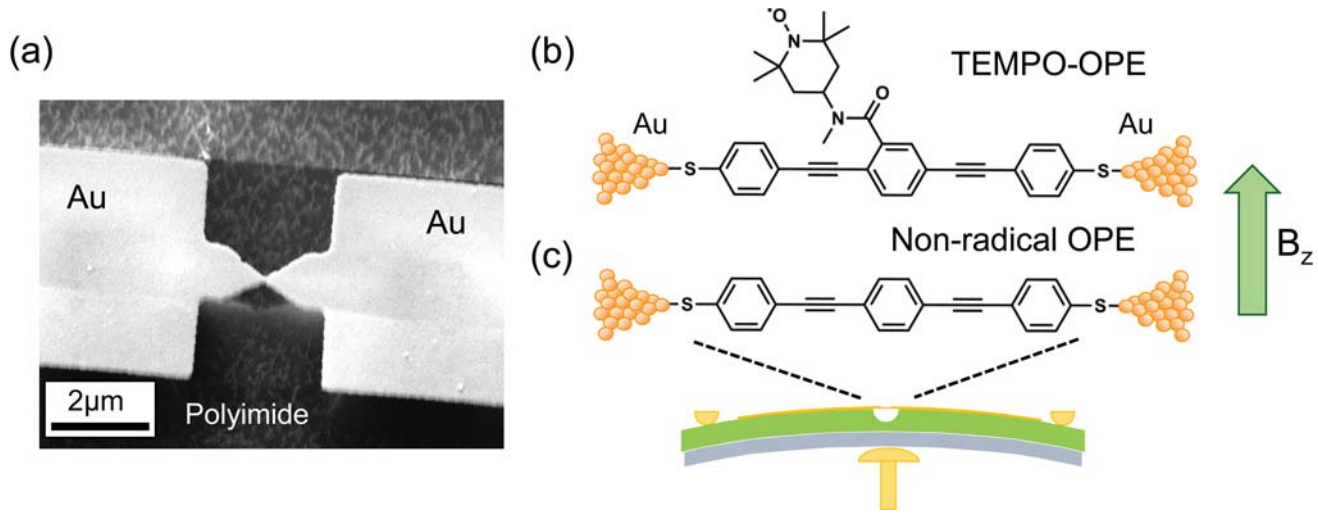

Figure 1. Experimental setup. (a) A scanning electron microscope image of a MCBJ sample with Au freestanding bridges. A schematic illustration of single molecule junctions for (b) TEMPO OPE and (c) pristine OPE. Magnetic fields are applied perpendicular to the sample plane for the charge transport measurements.

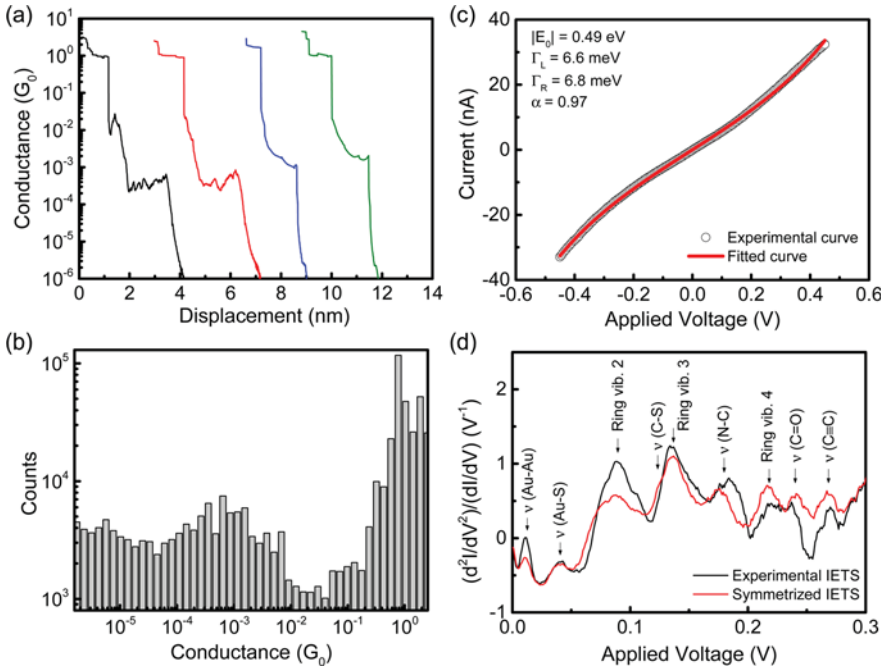

Figure 2. Transport properties of Au−TEMPO OPE−Au molecular junctions. (a) Conductance traces in breaking process of TEMPO OPE molecular junctions. (b) Conductance histograms of TEMPO OPE molecular junctions. (c) A typical $I-V$ characteristic of a TEMPO OPE single molecule junction. The solid red line indicates a fitting curve calculated with the single level model (eq 1). (d) Experimental and symmetrized IET spectra $(d^2I/dV^2)/(dI/dV)$ at a molecular junction. The red line is given by the point symmetric function, $(f(x) - f(-x))/2$. The respective vibration peaks are assigned with reference to IETS, infrared, and Raman spectroscopy measurements of OPE and TEMPO radical molecules.

yn 2 yl])phenyl]carbonyl}(methyl)amino] 2,2,6,6 tetramethyl piperidin 1 yl}oxidanyl (TEMPO OPE **1**), are placed on a freestanding gold (Au) bridge made with a standard lithography technique (Figure 1b).[29,30] The process used to synthesize the radical molecules and the details of the experimental procedures are described in the Supporting Information. A feature of the radical molecules is that they are composed of an OPE backbone molecule, which is archetypical in the field of molecular electronics and offers coherent charge transport between two electrodes through Au−S bonds.[31−33] In addition, the orbital of the unpaired electron on the TEMPO radical is not conjugated with the π orbitals of the OPE backbone molecule; that is, the radical part is considered to be electrically isolated from the main transport channel. This property makes it possible to preserve the localization of the unpaired electron on the molecules. Moreover, Kohn−Sham density functional theory (KS DFT) calculations (carried out in the absence of a magnetic field) suggest that the radical molecules bridging between Au electrodes have two possible configurations (see Figures S1−S5). In one structure, the TEMPO radical is oriented toward one of the thiols and can thus potentially interact directly with a Au electrode. This suggests that despite the electronic decoupling from the OPE backbone, the radical may affect charge transport under magnetic fields. Calculations

with Grimme's dispersion correction also imply that the sterical interaction between the TEMPO radical unit and the OPE backbone may be strong enough to induce a tilt of one of the phenyl rings (Figure S1–S4).

In this study, we observed considerably large positive MRs from TEMPO OPE molecules when a magnetic field was applied perpendicular to the samples. The change in resistance was more than an order of magnitude larger than that of the analogous nonradical OPE molecule (Figure 1c), obtained via deprotection of S,S′ [1,4 phenylenebis(ethyne 2,1 diyl 4,1 phenylene)]diethanethioate and investigated under the same conditions. Our detailed analysis of current–voltage (I–V) measurements and inelastic electron tunneling spectroscopy (IETS) measurements suggested that the large MR from radical molecules may be induced by a loss of coherence of the electron transport with increasing magnetic field amplitudes. These results imply that the unpaired electron may contribute to the localization of π orbitals in TEMPO OPE molecules, which would provide a new physical approach for tuning the charge transport via radical molecules.

First, we evaluated the fundamental charge transport properties through Au–TEMPO OPE–Au junctions without magnetic fields, complemented by conductance histograms and I–V and IETS measurements. All measurements were performed at a low temperature of 4.2 K. The single molecular junctions were formed by repeatedly breaking and reforming Au contacts. Figure 2a shows some typical opening curves of the junctions in the range of 3 to 10^{-6} G_0, where $G_0 = 2e^2/h$ is the conductance quantum, e is the elementary charge, and h is Planck's constant. Clear plateaus appeared in the range of 10^{-4} to 10^{-3} G_0 after breaking the Au single atom contacts. The lengths of the pronounced plateaus were estimated to be 1.5–2.0 nm, which is in good agreement with that of the OPE backbone (2.07 nm).[31,33] Subsequently we obtained the conductance histogram shown in Figure 2b. Here, the histogram was constructed from all opening traces of the junctions and shows a single, broad maximum at $6.0 \pm 3.8 \times 10^{-4}$ G_0. The conductance value is also close to those for OPE molecules with Au–S bonds ($3.7 \pm 2.0 \times 10^{-4}$ G_0 for our measurement (Figure S12) and $1.2–2.8 \times 10^{-4}$ G_0 for the values in literature).[31,33–35] Further statistical information on the experiments is summarized in the Supporting Information.

I–V measurements were carried out to obtain an insight into the charge transport mechanism of TEMPO OPE junctions. The I–V curves were analyzed with the single level model, which is widely used to describe the charge transport via π conjugated molecules despite the simplified assumption that the current is carried by one molecular orbital.[36–38] In this model, the I–V curve is given by eq 1 with the Landauer formula.

$$I(V) = \frac{2e}{h}\int_{-\infty}^{\infty} T(E,V)\left[f\left(E - \frac{eV}{2}\right) - f\left(E + \frac{eV}{2}\right)\right] dE \quad (1)$$

where e is the electron charge, h is Planck's constant, and $f(E)$ is the Fermi–Dirac distribution function. The transmission function, $T(E,V)$, is given by the Breit–Wigner formula in eqs 2 and 3.

$$T(E,V) = \frac{4\Gamma_L\Gamma_R}{[E - E_0(V)]^2 + [\Gamma_L + \Gamma_R]^2} \quad (2)$$

$$E_0(V) = E_0 + \left(\frac{\Gamma_L - \Gamma_R}{\Gamma_L + \Gamma_R}\right)\frac{eV}{2} \quad (3)$$

Here, E_0 indicates the energy of the current carrying molecular orbital (in general, the HOMO or the LUMO) relative to the Fermi energy, E_F, of the metal electrodes, which can adopt both signs, $E_0 > 0$ for the LUMO and $E_0 < 0$ for the HOMO. We note that the functional form of the resonance means that the sign of E_0 cannot be determined, i.e., strictly speaking, $|E_0|$ is determined by fitting eq 1 to the experimentally observed I–V curves. Γ_L and Γ_R represent coupling constants for the left and right electrodes, respectively. The degree of asymmetry in the coupling is defined by $\alpha = \Gamma_L/\Gamma_R$ or Γ_R/Γ_L, where the numerator has a smaller value than the denominator. The closer proximity of the highest occupied molecular orbital (HOMO, around −6.3 eV; see Figure S6) to the assumed Fermi level of −5 eV compared with the lowest occupied MO (LUMO; around −2.5 eV) suggests that it is reasonable to use such a single level model, but it should be kept in mind that the location of E_F cannot be determined with certainty from our calculations, as the description of metal–molecule interfaces is a challenge for DFT, and adsorbate layer effects are not taken into account by the theoretical description of a single molecule on which our analysis is based. The assumption of the single level model is further justified by the fact that transmission function is well described by a Lorentzian line shape close to the Fermi energy (see Figure S7).

We evaluated 130 I–V curves form TEMPO OPE junctions, of which 113 curves were well fitted by the single level model. Figure 2c shows a typical I–V curve for a contact with 7.4×10^{-4} G_0. The curve was well fitted by a model whose parameters were an energy level of $|E_0| = 0.49$ eV and coupling constants of $\Gamma_L = 6.6$ meV and $\Gamma_R = 6.8$ meV. The coupling symmetricity factor, $\alpha = \Gamma_L/\Gamma_R$, was calculated to be 0.97, revealing that the molecule is symmetrically connected to both electrodes. These estimated parameters agree well with those reported for OPE molecules ($|E_0| = 0.50 \pm 0.15$ eV, $\Gamma = 8.4 \pm 4.2$ meV).[33] The DFT calculations on the electronic structure of the TEMPO OPE and the local transmission contributions of the junctions suggest that the current flows through the OPE backbone in the TEMPO OPE molecule; the HOMO works as conductive channel (Figures S6–S9). For further information on the charge transport, a statistical analysis of the I–V curves is given in Figure S13.

IETS measurements were performed to identify excited vibrational modes for TEMPO OPE junctions. Here, we measured the spectra of 50 different junctions recorded on 2018 opening traces after complete reclosure of the junctions and on five samples. Figure 2d shows a representative IET spectrum with a positive bias voltage for a molecular junction and one that has been symmetrized by the following point symmetric function, $y = [f(x) - f(-x)]/2$. Here, the IET spectrum was symmetrized, and all of the peaks were observed at the same bias voltages in both the raw and symmetrized spectra.[38] In addition, the amplitude of the IETS signals (d^2I/dV^2) was normalized by that of dI/dV to compensate for the change in conductance. The spectrum over the entire voltage range is described in Figure S14. We assigned the pronounced peaks to specific vibrational modes in the TEMPO OPE molecules by comparison with those of OPE and the derivatives (Figure S15). We also referred to infrared and Raman spectroscopy measurements of TEMPO radical molecules for the assignment of N–C vibrations[39–41] and compared them

with vibrational spectra calculated by DFT (Figures S10 and S11). The detected vibrational peaks are summarized in Table S1. The detection of characteristic vibrational peaks in the TEMPO OPE molecules, e.g., N−C, C═O stretching modes, and benzene ring vibrations, provides further verification that the current passes through a single TEMPO OPE molecule.

We now turn to the discussion of the charge transport under a magnetic field, namely MR measurements and the Kondo resonance effects on single molecule junctions of the radical. Figure 3 shows typical MR curves for TEMPO OPE junctions

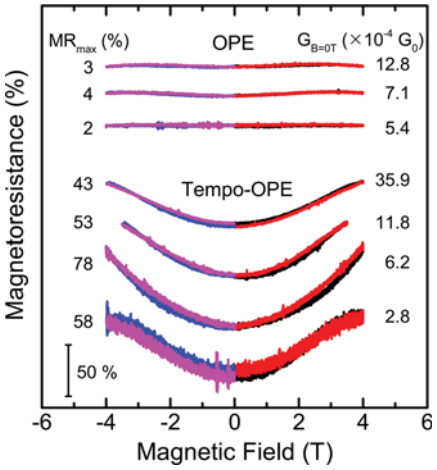

Figure 3. Magnetoresistance curves from TEMPO OPE molecular junctions. For comparison, the curves from pristine OPE are shown in the same figure and with the same scale. The magnetic fields were applied up to ±4 T, starting at 0 T, increasing to +4 T (black), returning to 0 T (red), decreasing to −4 T (blue), and finally returning to 0 T (magenta). The resistances are shown as $[R(B) - R(0)] \times 100/R(0)$ (%), where $R(B)$ and $R(0)$ are respective resistances at maximum magnetic fields and at 0 T. Please note that individual curves are shifted vertically for better visibility.

in different conductance ranges, where magnetic fields were applied perpendicular to the sample plane. The magnetic field sweep rate was fixed at 400 mT/min. The resistance was measured at a DC voltage of 30 mV to be close to the linear regime but outside possible zero bias anomalies and to avoid current driven rearrangements during measurements. For comparison, MR curves obtained from OPE junctions are also displayed in the same figure. We observed remarkably large positive MRs, and the value is at least 1 order of magnitude larger than that of nonradical OPE molecules, despite the fact that both molecules have a similar molecular structure. The magnetoresistance histogram from TEMPO OPE and OPE junctions is given in Figure S16. Here, the MRs were measured at 23 junctions for TEMPO OPE, out of which 17 junctions (74%) indicated large MR values of more than 16% at 4 T. The maximum value was 287%. The other junctions revealed the same shape of MR curves; however, the amplitudes were 2−6%. The average value of all observed MRs was estimated to be 43.7% at 4 T, in contrast to 2.2% for OPE junctions. In addition, it is notable that the MR curves from TEMPO OPE junctions revealed a saturation and subsequent decrease at a high magnetic field of 4 T to 6 T (Figures S17a and S18). Similar behavior is also observed for OPE and Au atom junctions (Figure S17b,c), which shows that the shape of the MR traces is not a unique feature of TEMPO OPE junctions.

In some of the dI/dV curves, we observe zero bias anomalies that resemble Kondo resonances, as recently reported by Frisenda et al. for single molecule junctions of polychloro triphenylmethyl (PTM), a molecule bearing a radical in its conduction path at very low temperature.[24] In our case, the width of the zero bias anomaly is much larger than that reported in ref 24 and would correspond to a Kondo temperature of ∼360 K. Furthermore, the peaks did not split, even by the application of magnetic fields up to 5 T (see Figure S19). This result is in agreement with results from the DFT calculations, which suggest that the TEMPO radical part is electrically only very weakly coupled to the main transport channel (Figures S8 and S9). Therefore, we do not expect to observe the Kondo effect in the TEMPO OPE junctions. Measurements in a wider temperature range and at much higher magnetic fields would be required to verify the presence or absence of the Kondo effect.

Next, we discuss possible origins of the large MR of the TEMPO OPE junctions. Such huge MRs have not been reported in single molecule junctions to date. For example, in the study by Frisenda et al. on PTM junctions,[24] no MR measurements were reported. Recently, some examples have been reported on charge transport through organic materials under magnetic fields. Sugawara et al. demonstrated negative MRs for Au nanoparticles linked by a nitronyl nitroxide radical molecule, where the current was assumed to flow through radical molecules bridging between Au particles.[42,43] The negative MRs are explained by a reduction of spin flip scattering. This is because magnetic fields define a preferable orientation for localized spins, and therefore, the spin flip scattering of conductive electrons is restricted by an increasing magnetic field. Meanwhile, in our case, only positive MRs were visible, and therefore, this spin flip scattering model is unlikely. In addition, Au surfaces have been reported to be magnetized through Au−S bonds, which may affect the charge transport through a bridged molecule.[44,45] On the one hand, such a spin polarization effect is unlikely to dominantly contribute to the variation in MRs because only a small change in the MRs was observed for OPE junctions, despite the fact that the molecule has the same Au−S bonds. On the other hand, a facilitation of Au−S spin polarization through the presence of the radical cannot be fully excluded. Furthermore, the overall transmission calculations clarify that the TEMPO OPE molecules do not work effectively as spin filters because the radical parts are located far from the backbone molecules, resulting in virtually equal transmission probabilities for majority and minority spins (Figure S7). The same conclusion has been pointed out in the theoretical study of the spin filtering effects of stable radical groups, including nitronyl nitroxide and *tert* butylphenylnitr oxide radicals, which are similar to that of our molecule.[46,47] However, markedly large positive MRs (10% at 10 mT) have been demonstrated in pure organic thin films and molecular wires with nonmagnetic electrodes such as Au and tin doped indium oxide electrodes.[48−50] In these studies, the positive MRs are interpreted by the hyperfine interaction between conductive electrons and nuclear spins of molecules during the electron hopping conduction, whereas the MRs appeared at the magnetic field of a few Tesla in our case, and the amplitude is much larger than that of hyperfine fields of typical organic molecules (2−6 mT).[48,49] The Zeeman splitting of molecular orbitals also cannot explain the MRs obtained from TEMPO OPEs because of the marginal change in MRs for OPEs. Hence, a different mechanism from those already proposed for organic

molecules is required to explain the origin of the positive MR in our study.

To understand why such a huge MR appeared for TEMPO OPE molecules, we performed $I-V$ measurements under different magnetic fields (Figure S20a). The $I-V$ curves were analyzed with the single level model described by eqs 1−3. Panels a and b of Figure 4 show the changes in the conductance

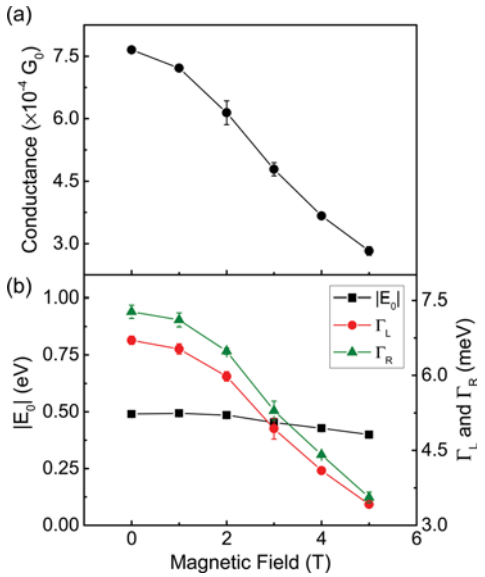

Figure 4. Magnetic field dependence of the charge transport through an Au/TEMPO OPE/Au single molecule junction. Change in (a) conductance and (b) energy level position, $|E_0|$, and coupling constants, Γ_L and Γ_R, as a function of magnetic field.

and fitting parameters, $|E_0|$, Γ_L, and Γ_R, as a function of the magnetic field. The conductance was reduced by 62% when the magnetic field was increased to 5 T, corresponding to a 162% positive MR. This conductance change is caused by a strong decrease in the coupling constants, which dropped markedly to almost 50% as the magnetic field increased to 5 T. In contrast, the slight decrease in the energy level from 0.5 to 0.4 eV with increasing magnetic field reveals a certain improvement of the level alignment between the molecular orbital and the Fermi level of the electrodes, and this would result in an increase of conductance if the coupling constants were independent of the magnetic field. A similar tendency was observed in the other junctions. Another example is shown in Figure S21. In the junction, the change in $|E_0|$ was estimated to be 3%. In contrast, the variations in Γ_L and Γ_R amounted to 20%. These results clarify that the huge MR for TEMPO OPE molecules is dominantly induced by a reduction in the coupling strength between the current carrying molecular orbital and the electrodes. For comparison, equivalent experiments were made with OPE molecules. No variation was observed in $I-V$ curves with magnetic fields (Figure S20b). These results indicate that the unpaired electron plays an essential role in the change in the orbital coupling between molecules and electrodes.

Here, we consider possible origins for the observed reduction in the coupling strength under magnetic fields. Prior to the discussion, it should be noted that the junction region would be surrounded by many molecules because of their deposition from a solution, and their possible contribution to the charge transport via the bridged molecule should not be ignored, although only one molecule is electrically contacted to both sides of the electrodes.[16,51] A possible mechanism would be the change of conformation of a molecule under a magnetic field. Structural changes caused by magnetic fields are well known in transition metal complexes, and the effect is employed to control molecular orientation in grown films.[52,53] Here, the magnetic moments of surrounding molecules might induce a magnetic distortion of the electrodes. The second reason could be a variation of the electronic structure, e.g., by narrowing the Breit−Wigner resonance, which might be caused by a change of the π orbital system induced by the attached radical group. Another possible electronic effect would be the loss of the phase coherence of the conduction electrons in the metal electrodes. Because constructive quantum interference contrib utes to the transport, the reduction of phase coherence might cause an increase of the resistance.[54,55] Because similar changes of $|E_0|$, Γ_L, and Γ_R were visible when the molecules were subjected to tensile stress by gradually displacing the electrodes (Figure S22), an additional experiment is required to dispel this effect. To this end, we evaluated the development of the IETS with magnetic fields and compared the result with the development with stretching because the IET signals are sensitive to changes in molecular vibrations and intensities caused by changes in both the geometrical and electronic structures.

Figure 5a shows symmetrized IET spectra in different magnetic fields varying from 0 to 5 T. The IETS peak positions remained almost unchanged, but a clear attenuation of the peak intensities was visible. This result manifests that the change of the electronic structure in the molecule is more dominant than that of the molecular conformation. Figure 5b shows the

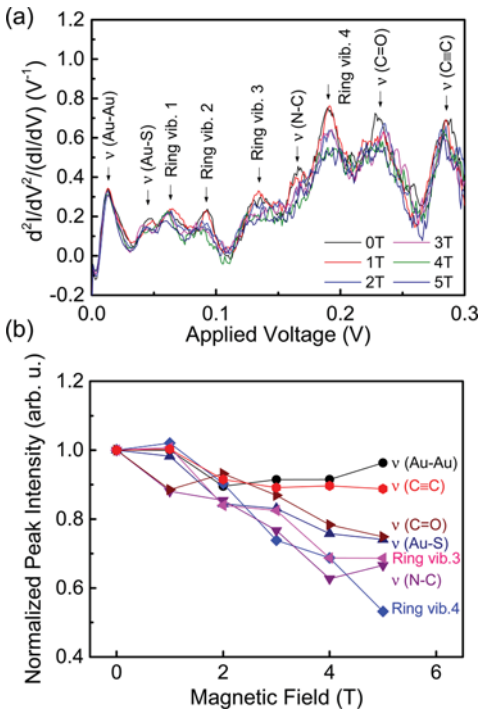

Figure 5. Magnetic field dependence of the inelastic transport properties of an Au/TEMPO OPE/Au junction. (a) Symmetrized IET spectra in different magnetic fields up to 5 T. (b) The change in peak intensities for representative vibration modes as a function of magnetic field. Here, the intensities are normalized to those without a magnetic field.

variation in the intensities of representative vibrational peaks. Here, the peak intensities are normalized by those without a magnetic field. All of the molecular vibrational peaks were suppressed by increasing the magnetic field. In particular, the peak intensities for benzene ring vibrations and the side group (υ(N−C) and υ(C═O)) were definitely reduced. The Au phonon mode peak also decreased, although the variation is quite small (less than 10%). Such suppression of the vibration peaks was not seen in the IET spectra for OPE junctions (Figure S24). The corresponding peak intensities fluctuated with a deviation of only 20%, regardless of magnetic fields.

In addition, a very distinct behavior was observed when a molecular junction was stretched (Figure S22). We observed a pronounced increase of the peak intensity of the longitudinal optical phonon of the Au−Au bonds, which is a typical behavior of atomic chains and molecular junctions. A similar tendency was demonstrated in our previous results on Au 1,6 hexanedithiol molecule Au junctions.[38] No such large change in Au−Au optical phonons was visible when the magnetic field was increased. In addition, the peak intensities attributed to the stretching vibration of C≡C bonds and benzene ring vibrations were enhanced by increasing the electrode displacement, while the peak positions remain unchanged.

These differences provide clear evidence that the conductance reduction in a magnetic field is not caused by a change in geometry of the junctions but by a variation in the electronic structure. To be more specific, we suggest the following model. The magnetic field confined electronic wave functions, as known in mesoscopic physics.[56] In the present system, this localization has a 2 fold effect; first, it confines the π−orbitals of the molecule, thereby reducing their coupling with the conduction electrons of the electrodes. Second, the magnetic field acts on the conduction electrons of the metal electrodes themselves, leading to dephasing, as known from, e.g., weak localization studies.[54,55] Although no clear weak localization feature is visible in the magnetoconductance due to its small amplitude, this loss of decoherence would be reflected in the reduction of the IET amplitudes. However, both effects should also be active in OPEs without the radical. Therefore, we consider that the presence of the localized magnetic moments of the unpaired radical electron might amplify the dephasing effect, the localization effect, or both. This amplification idea is supported by the observation of similar functional shapes of the MR traces of the TEMPO OPE and the pristine OPE junctions. In this respect, our DFT calculations suggest that the unpaired electrons may be located spatially quite close to the Au surface, that the TEMPO radical unit may induce a tilt of the phenyl ring in the OPE backbone in the initial state, or both. Thus, the radical part may influence conductance although it is considered to be electronically decoupled from the π system of the OPE backbone (Figures S1−S6). Such specific configurations may facilitate the dephasing of conduction electrons in Au electrodes by the local magnetic moments and the confinement of the π orbitals in the radical molecules under magnetic fields. Further investigation is necessary to clarify the mechanism.

In summary, we investigated electron transport through single TEMPO OPE molecular junctions under magnetic fields by a MCBJ technique at 4.2 K. Substantially large positive MRs of 16 to 278% were observed at 4 T, in contrast to those of nonradical OPE molecules, which exhibited MRs in the range of 2−4%. A detailed analysis based on I−V and IETS measurements with magnetic fields provided clear evidence that the large MRs for TEMPO OPE were caused by reducing the coupling of the current carrying molecular orbital with the metal electrodes. These results suggest that the confinement of π−orbitals in magnetic fields may be caused or enhanced by the magnetic moment of an unpaired electron on the TEMPO OPE molecules. Therefore, our finding offers a possible new approach to manipulate the charge transport in organic radical molecules.

AUTHOR INFORMATION

Corresponding Authors

*R.H. e mail: HAYAKAWA.Ryoma@nims.go.jp.

*E.S. e mail: elke.scheer@uni.konstanz.de.

Notes

The authors declare no competing financial interest.

ACKNOWLEDGMENTS

This research was supported by the World Premier International Center (WPI) for Materials Nanoarchitectonics (MANA) of the National Institute for Materials Science

(NIMS) (Tsukuba, Japan) and the Deutsche Forschungsgemeinschaft (DFG) through SFB767. M.S.Z. and C.H. thank the DFG for funding through SFB668. We thank P. Selvanathan, L. Norel, and S. Rigaut for providing the unsubstituted OPE molecule. We are indebted to S. Rigaut, C. A. Stafford, and the members of the SFB discussion group on Molecular Electronics for helpful discussions and insightful remarks on the manuscript.

REFERENCES

(1) Rocha, A. R.; García Suárez, V. M.; Bailey, S. W.; Lambert, C. J.; Ferrer, J.; Sanvito, S. *Nat. Mater.* **2005**, *4*, 335−339.
(2) Schmaus, S.; Bagrets, A.; Nahas, Y.; Yamada, T.; Bork, A.; Bowen, M.; Beaurepaire, E.; Evers, F.; Wulfhekel, W. *Nat. Nanotechnol.* **2011**, *6*, 185−189.
(3) Urdampilleta, M.; Klyatskaya, S.; Cleuziou, J. P.; Ruben, M.; Wernsdorfer, W. *Nat. Mater.* **2011**, *10*, 502−506.
(4) Miyamachi, T.; Gruber, M.; Davesne, V.; Bowen, M.; Boukari, S.; Joly, L.; Scheurer, F.; Rogez, G.; Yamada, T.; Ohresser, P.; Beaurepaire, E.; Wulfhekel, W. *Nat. Commun.* **2012**, *3*, 938.
(5) Harzmann, G. D.; Frisenda, R.; van der Zant, H. S. J.; Mayor, M. *Angew. Chem., Int. Ed.* **2015**, *54*, 1−7.
(6) Rakhmilevitch, D.; Sarkar, S.; Bitton, O.; Kronik, L.; Tal, O. *Nano Lett.* **2016**, *16*, 1741−1745.
(7) Aragones, A. C.; Aravena, D.; Cerda, J. I.; Acis Castillo, Z.; Li, H.; Real, J. A.; Sanz, F.; Hihath, J.; Ruiz, E.; Diez Perez, I. *Nano Lett.* **2016**, *16*, 218−226.
(8) Gomberg, M. *J. Am. Chem. Soc.* **1900**, *22*, 757−771.
(9) Simão, C.; Mas Torrent, M.; Crivillers, N.; Lloveras, V.; Artés, J. M.; Gorostiza, P.; Veciana, J.; Rovira, C. *Nat. Chem.* **2011**, *3*, 359−364.
(10) Ratera, I.; Veciana, J. *Chem. Soc. Rev.* **2012**, *41*, 303−349.
(11) Sanvito, S. *Nat. Mater.* **2007**, *6*, 803−804.
(12) Pramanik, S.; Stefanita, C. G.; Patibandla, S.; Bandyopadhyay, S.; Garre, K.; Harth, N.; Cahay, M. *Nat. Nanotechnol.* **2007**, *2*, 216−219.
(13) Tamura, M.; Nakazawa, Y.; Shiomi, D.; Nozawa, K.; Hosokoshi, Y.; Ishikawa, M.; Takahashi, M.; Kinoshita, M. *Chem. Phys. Lett.* **1991**, *186*, 401−404.
(14) Grynóva, G.; Coote, M. L.; Corminboeuf, C. *WIREs Comput. Mol. Sci.* **2015**, *5*, 440−459.
(15) Komatsu, H.; Matsushita, M. M.; Yamamura, S.; Sugawara, Y.; Suzuki, K.; Sugawara, T. *J. Am. Chem. Soc.* **2010**, *132*, 4528−4529.
(16) Lloveras, V.; Badetti, E.; Wurst, K.; Chechik, V.; Veciana, J.; Vidal Gancedo. *Chem. Eur. J.* **2016**, *22*, 1805−1815.
(17) Parks, J. J.; Champagne, A. R.; Costi, T. A.; Shum, W. W.; Pasupathy, A. N.; Neuscamman, E.; Flores Torres, S.; Cornaglia, P. S.; Aligia, A. A.; Balseiro, C. A.; Chan, G. K. L.; Abruña, H. D.; Ralph, D. C. *Science* **2010**, *328*, 1370−1373.
(18) Komeda, T.; Isshiki, H.; Liu, J.; Zhang, Y. F.; Lorente, N.; Katoh, K.; Breedlove, B. K.; Yamashita, M. *Nat. Commun.* **2011**, *2*, 217.
(19) Wagner, S.; Kisslinger, F.; Ballmann, S.; Schramm, F.; Chandrasekar, R.; Bodenstein, T.; Fuhr, O.; Secker, D.; Fink, K.; Ruben, M.; Weber, H. B. *Nat. Nanotechnol.* **2013**, *8*, 575−579.
(20) Schwarz, F.; Kastlunger, G.; Lissel, F.; Egler Lucas, C.; Semenov, S. N.; Venkatesan, K.; Berke, H.; Stadler, R.; Lörtscher, E. *Nat. Nanotechnol.* **2016**, *11*, 170−176.
(21) Zhang, Y. H.; Kahle, S.; Herden, T.; Stroh, C.; Mayor, M.; Schlickum, U.; Ternes, M.; Wahl, P.; Kern, K. *Nat. Commun.* **2013**, *4*, 2110.
(22) Liu, J.; Isshiki, H.; Katoh, K.; Morita, T.; Breedlove, B. K.; Yamashita, M.; Komeda, T. *J. Am. Chem. Soc.* **2013**, *135*, 651−658.
(23) Müllegger, S.; Rashidi, M.; Fattinger, M.; Koch, R. *J. Phys. Chem. C* **2013**, *117*, 5718−5721.
(24) Frisenda, R.; Gaudenzi, R.; Franco, C.; Mas Torrent, M.; Rovira, C.; Veciana, J.; Alcon, I.; Bromley, S. T.; Burzurí, E.; van der Zant, H. S. J. *Nano Lett.* **2015**, *15*, 3109−3114.
(25) Jo, M. H.; Grose, J. E.; Baheti, K.; Deshmukh, M. M.; Sokol, J. J.; Rumberger, E. M.; Hendrickson, D. N.; Long, J. R.; Park, H.; Ralph, D. C. *Nano Lett.* **2006**, *6*, 2014−2020.
(26) Kahle, S.; Deng, Z.; Malinowski, N.; Tonnoir, C.; Forment Aliaga, A.; Thontasen, N.; Rinke, G.; Le, D.; Turkowski, V.; Rahman, T. S.; Rauschenbach, S.; Ternes, M.; Kern, K. *Nano Lett.* **2012**, *12*, 518−521.
(27) Warner, B.; El Hallak, F.; Prüser, H.; Sharp, J.; Persson, M.; Fisher, A. J.; Hirjibehedin, C. F. *Nat. Nanotechnol.* **2015**, *10*, 259−263.
(28) Heinrich, B. W.; Braun, L.; Pascual, J. I.; Franke, K. J. *Nano Lett.* **2015**, *15*, 4024−4028.
(29) Kim, Y.; Pietsch, T.; Erbe, A.; Belzig, W.; Scheer, E. *Nano Lett.* **2011**, *11*, 3734−3738.
(30) Kim, Y.; Hellmuth, T. J.; Bürkle, M.; Pauly, F.; Scheer, E. *ACS Nano* **2011**, *5*, 4104−4111.
(31) Wu, S.; González, M. T.; Huber, R.; Grunder, S.; Mayor, M.; Schönenberger, C.; Calame, M. *Nat. Nanotechnol.* **2008**, *3*, 569−574.
(32) Fu, X. X.; Zhang, R. Q.; Zhang, G. P.; Li, Z. L. *Sci. Rep.* **2014**, *4*, 6357.
(33) Frisenda, R.; Tarkuç, S.; Galán, E.; Perrin, M. L.; Eelkema, R.; Grozema, F. C.; van der Zant, H. S. J. *Beilstein J. Nanotechnol.* **2015**, *6*, 1558−1567.
(34) Hong, W.; Li, H.; Liu, S. X.; Fu, Y.; Li, J.; Kaliginedi, V.; Decurtins, S.; Wandlowski, T. *J. Am. Chem. Soc.* **2012**, *134*, 19425−19431.
(35) Huber, R.; González, M. T.; Wu, S.; Langer, M.; Grunder, S.; Horhoiu, V.; Mayor, M.; Bryce, M. R.; Wang, C.; Jitchati, R.; Schönenberger, C.; Calame, M. *J. Am. Chem. Soc.* **2008**, *130*, 1080−1084.
(36) Büttiker, M.; Imry, Y.; Landauer, R.; Pinhas, S. *Phys. Rev. B: Condens. Matter Mater. Phys.* **1985**, *31*, 6207−6215.
(37) Huisman, E. H.; Guédon, C. M.; van Wees, B. J.; van der Molen, S. J. *Nano Lett.* **2009**, *9*, 3909−3913.
(38) Kim, Y.; Song, H.; Strigl, F.; Pernau, H. F.; Lee, T.; Scheer, E. *Phys. Rev. Lett.* **2011**, *106*, 196804.
(39) Kushmerick, J. G.; Lazorcik, J.; Patterson, C. H.; Shashidhar, R.; Seferos, D. S.; Bazan, G. C. *Nano Lett.* **2004**, *4*, 639−642.
(40) Kula, M.; Jiang, J.; Luo, Y. *Nano Lett.* **2006**, *6*, 1693−1698.
(41) Rintoul, L.; Micallef, A. S.; Bottle, S. E. *Spectrochim. Acta, Part A* **2008**, *70*, 713−717.
(42) Sugawara, T.; Minamoto, M.; Matsushita, M. M.; Nickels, P.; Komiyama, S. *Phys. Rev. B: Condens. Matter Mater. Phys.* **2008**, *77*, 235316.
(43) Nickels, P.; Matsushita, M. M.; Minamoto, M.; Komiyama, S.; Sugawara, T. *Small* **2008**, *4*, 471−475.
(44) Nealon, G. L.; Donnio, B.; Greget, R.; Kappler, J. P.; Terazzi, E.; Gallani, J. L. *Nanoscale* **2012**, *4*, 5244−5258.
(45) Gonzalez, C.; Simón Manso, Y.; Marquez, M.; Mujica, M. *J. Phys. Chem. B* **2006**, *110*, 687−691.
(46) Herrmann, C.; Solomon, G. C.; Ratner, M. A. *J. Am. Chem. Soc.* **2010**, *132*, 3682−3684.
(47) Herrmann, C.; Solomon, G. C.; Ratner, M. A. *J. Chem. Phys.* **2011**, *134*, 224306.
(48) Sheng, Y.; Nguyen, T. D.; Veeraraghavan, G.; Mermer, Ö.; Wohlgenannt, M.; Qiu, S.; Scherf, U. *Phys. Rev. B: Condens. Matter Mater. Phys.* **2006**, *74*, 045213.
(49) Giro, R.; Rosselli, F. P.; dos Santos Carvalho, R.; Capaz, R. B.; Cremona, M.; Achete, C. A. *Phys. Rev. B: Condens. Matter Mater. Phys.* **2013**, *87*, 125204.
(50) Mahato, R. N.; Lülf, H.; Siekman, M. H.; Kersten, S. P.; Bobbert, P. A.; de Jong, M. P.; De Cola, L.; van der Wiel, W. G. *Science* **2013**, *341*, 257−260.
(51) Zhang, Z.; Berg, A.; Levanon, H.; Fessenden, R. W.; Meisel, D. *J. Am. Chem. Soc.* **2003**, *125*, 7959−7963.
(52) Kolotovska, V.; Friedrich, M.; Zahn, D. R. T.; Salvan, G. *J. Cryst. Growth* **2006**, *291*, 166−174.
(53) Takami, S.; Furumi, S.; Shirai, Y.; Wakayama, Y.; Sakka, Y. *J. Mater. Chem.* **2012**, *22*, 8629−8633.

(54) Lee, P. A.; Stone, A. D.; Fukuyama, H. *Phys. Rev. B: Condens. Matter Mater. Phys.* **1987**, *35*, 1039.
(55) Washburn, S.; Webb, R. A. *Adv. Phys.* **1986**, *35*, 375−422.
(56) Mikoshiba, N. *Phys. Rev.* **1962**, *127*, 1962−1969.